Manufacturing Technologies and Applications
MATECA

Machine Learning-Based Surface Roughness Prediction in Eco-Friendly Milling of AISI 420 Stainless Steel

Yusuf Furkan Yapan[1,*], Anuj Kumar Jha[2], Navneet Khanna[2], Alper Uysal[1]

[1] *Yildiz Technical University, Department of Mechanical Engineering, Istanbul, 34349, Türkiye*
[2] *Advanced Manufacturing Laboratory, Institute of Infrastructure Technology Research and Management, Ahmedabad 380026, India*

ABSTRACT

Although martensitic stainless steels (MSS) are widely used due to their superior mechanical and chemical properties, their poor machinability can lead to surface quality degradation. Therefore, in addition to improving the surface quality of the material using advanced machining methods, it is important to predict the surface quality to increase efficiency, reduce waste, and prevent faulty functionality. In this study, surface roughness was predicted for the first time using various machine learning models such as, polynomial regression, support vector regression, decision tree regression, random forest regression, and k-nearest neighbors regression, depending on the cutting condition, minimum quantity lubrication (MQL) flow rate, nanoparticle concentration, cutting tool coating, and cutting temperature in sustainable milling of AISI 420 MSS using the MQL method with multi-walled carbon nanotube (MWCNT)-reinforced nanofluid (NMQL). Titanium nitride (TiN)-coated tungsten carbide (WC) cutting tool, NMQL method containing 0.15 wt.% MWCNT and 40 mL/h MQL flow rate improved the cutting temperature and surface roughness by 25.3% and 49.9%, respectively, compared to dry cutting condition with the uncoated WC cutting tool. he K-nearest neighbors regression model achieved the highest predictive accuracy for surface roughness, with a coefficient of determination (R^2) of 0.9789, outperforming the other evaluated machine learning approaches.

Keywords: *Machine learning, Martensitic stainless steel, MQL, Nanofluid, Surface roughness prediction*

AISI 420 Paslanmaz Çeliğin Çevre Dostu Frezelenmesinde Makine Öğrenmesi Tabanlı Yüzey Pürüzlülüğü Tahmini

ÖZET

Martenzitik paslanmaz çelikler, üstün mekanik ve kimyasal özellikleri nedeniyle yaygın olarak kullanılmalarına rağmen, zayıf işlenebilirlik özellikleri yüzey kalitesinde bozulmalara yol açabilmektedir. Bu nedenle, gelişmiş talaşlı imalat yöntemleri kullanılarak malzemenin yüzey kalitesinin iyileştirilmesinin yanı sıra; verimliliğin artırılması, israfın azaltılması ve hatalı fonksiyonların önlenmesi amacıyla yüzey kalitesinin önceden tahmin edilmesi büyük önem taşımaktadır. Bu çalışmada, çok duvarlı karbon nanotüp (ÇDKNT) takviyeli nanoakışkan içeren minimum miktarda yağlama (NMMY) yöntemi kullanılarak sürdürülebilir frezeleme koşullarında işlenen AISI 420 martenzitik paslanmaz çeliğin yüzey pürüzlülüğü, kesme koşulu, MMY debisi, nanoparçacık konsantrasyonu, kesici takım kaplaması ve kesme sıcaklığına bağlı olarak polinomsal regresyon, destek vektör regresyonu, karar ağacı regresyonu, rastgele orman regresyonu ve k-en yakın komşu regresyonu gibi çeşitli makine öğrenmesi modelleri kullanılarak ilk kez tahmin edilmiştir. Titanyum nitrür (TiN) kaplamalı tungsten karbür (WC) kesici takım ile birlikte %0,15 (ağırlıkça) ÇDKNT içeren ve 40 mL/saat MMY debisine sahip NMMY yöntemi, kaplamasız WC kesici takım kullanılan kuru kesme koşullarına kıyasla kesme sıcaklığını ve yüzey pürüzlülüğünü sırasıyla %25,3 ve %49,9 oranında iyileştirmiştir. K-en yakın komşular regresyon modeli, 0,9789'luk belirleme katsayısı (R^2) ile yüzey pürüzlülüğü için en yüksek tahmin doğruluğunu elde ederek değerlendirilen diğer makine öğrenme yaklaşımlarından daha iyi performans göstermiştir.

Anahtar Kelimeler*: Makine öğrenmesi, Martenzitik paslanmaz çelik, MQL, Nanoakışkan, Yüzey pürüzlülüğü tahmini*

1. INTRODUCTION

Martensitic stainless steels (MSS) are chromium-containing stainless steels (SS) (defined by a chromium content over 12% [1]) having a low carbon content, a high chromium concentration, and a body-centered cubic crystalline structure [2]. 400-series MSSs, such as AISI 410 and AISI 420, are frequently employed in many industries due to their corrosion resistance, wear resistance, hardness, and mechanical properties [1, 2]. However, the material's machinability is poor due to low thermal conductivity, high work hardening, and the

*Corresponding author, e-mail: yapan@yildiz.edu.tr

Received 29.01.2026; Accepted 14.04.2026
https://doi.org/10.52795/mateca.1872574
To cite this article: Y.F. Yapan, A.K. Jha, N. Khanna, A. Uysal, Machine Learning-Based Surface Roughness Prediction in Eco-Friendly Milling of AISI 420 Stainless Steel, Manufacturing Technologies and Applications 7(1)(2026) 43-60.

built-up edge (BUE) formation [3]. These poor properties make the material difficult to machine and negatively affect the surface quality.

Certain researchers have undertaken investigations on the machining of MSSs utilizing a variety of tool coatings under dry-cutting conditions [4, 5]. This is done in order to address the issue that has been brought up with the researchers. On the other hand, when it comes to the machining of SSs, the utilization of cutting fluid is unavoidable. This is due to the fact that coated tools do not offer the appropriate surface finish quality when operated under dry cutting conditions. In spite of the fact that the utilization of cutting fluid results in an enhancement of surface quality, it actually runs counter to the concept of sustainability, which is one of the most significant realities of the present day [6]. As a result of this, researchers are directing their attention toward the minimum quantity lubrication (MQL) method, which is a chip removal process that is less harmful to the environment. According to Babu and Manimaran [7], who conducted an investigation into the machining of MSSs using the MQL method, they found that the MQL method reduced the surface roughness of AISI 410 alloy by 51% and 9%, respectively, when the turning was performed under dry and wet cutting circumstances. In addition, Elmunafi et al. [8] discovered that raising the cutting speed and feed in the process of machining AISI 420 alloy resulted in an increase in the surface roughness improvement effect of MQL in comparison to the dry cutting condition. By employing mono and hybrid nanofluids containing MWCNT, MoS2, and Al2O3 in the MQL method, Yıldırım et al. [9] showed their ability to enhance the surface quality during the milling process of AISI420 alloy. When it comes to surface roughness and topography, it has been found that the optimum results may be achieved by utilizing Al_2O_3 and MoS_2 nanoparticles in a ratio of two to one. In the machining of MSSs, it has been noted that the surface quality can be improved by the use of MQL and nanofluid MQL (N-MQL) approaches. This is something that can be seen in the literature review that was presented earlier. On the other hand, the surface quality is affected by a number of aspects in addition to the lubrication and cooling method that is utilized [10, 11]. These include MQL parameters, cutting fluid and material properties, machining parameters, and cutting tool coating conditions.

There is a low level of efficiency in decision-making and a low level of surface quality in machining control since the majority of enterprises in the industry rely on the knowledge of machine operators to manage the surface quality of machined parts [12]. This circumstance results in waste, problems with functionality, and unhappiness among customers, particularly in the case of workpieces that have a high added value [13]. For these reasons, the utilization of advanced sensor systems plays a significant role in the accomplishment of advanced processing features, such as reduced labor, errors, production time, and so on, and it also satisfies the requirements of Industry 4.0 [14]. On the other hand, machine learning models that are based on artificial intelligence (AI) need to be utilized in order to process the data that is acquired from sensors in a timely and accurate manner and to forecast the continuation of the process [15]. The existing body of research on the prediction of surface roughness makes use of a number of studies that focus on machine learning (ML) as well as deep learning (DL), which is a sub-branch of ML [16, 17]. Although there are studies that successfully predict surface roughness using DL, it is less applicable to industrial settings than traditional ML models due to the fact that it requires a large amount of data, requires a high amount of computational power, takes a long time to train the model, poses the risk of overfitting, is difficult to tune hyperparameters, and lacks interpretability and transparency [18, 19]. In light of this, the present study aimed to evaluate the performance of ML approaches for surface roughness prediction. These methods are more easily applied in industrial settings and require less complexity.

The surface roughness was predicted by Prakasvudhisarn et al. [20] using support vector regression (SVR), which was superior to the performance of artificial neural networks (ANN). The surface roughness was then adjusted by combining SVR with particle swarm optimization (PSO). The surface roughness that was achieved following the turning process was predicted by Jurkovic et al. [21] using SVR, ANN, and polynomial regression (PR) models, with an error rate of 7.69%, 9.87%, and 7.52%, respectively. Classical regression, SVR, and ANN were employed in the research carried out by Yeganefar [22] to predict the surface roughness that was obtained with the inputs of cutting speed, feed, depth of cut, and cutting tool coating. The results of the study showed that the employment of ANN produced the best results. Surface roughness prediction was accomplished by Nguyen et al. [23] through the utilization of ANN, SVR, Cat Boost Regression (CAT), Gradient Boosting Regression (GBR), Decision Tree Regression (DT), and Extreme Gradient Boosting Regression (XGB). The XGB and CAT models were able to make the most accurate forecasts as a consequence of this. When it came to surface roughness prediction, Nguyen et al. [24] conducted a different study in which they utilized linear regression (LR), SVR, GBR, and ANN. They discovered that SVR and ANN were the most effective approaches. Zhang et al. [25] utilized ANN and Gaussian process regressions (GPR) models in order to forecast surface roughness in turning brass material. The surface roughness was predicted based on process characteristics such as cutting speed, feeding, and depth of cut. The prediction accuracy of GPR was 35.51%

higher than that of ANN. In the same vein, Motta et al. [26] came to the conclusion that GPR offers a more accurate forecast than RF when it comes to predicting surface roughness in the process of machining tool steel. Nevertheless, in this particular investigation, more than just cutting parameters were provided as input to machine learning models; cutting forces, accelerations, and temperatures were all included. SVM, GPR, adaptive neuro-fuzzy inference system (ANFIS), and ANN models were utilized by Adizue et al. [27] in order to correctly forecast the surface roughness of AISI D2 alloy turning. This was accomplished by utilizing the process parameters. When turning 4140 steel, Asilturk et al. [28] used the ANFIS model to make a prediction about the surface roughness, and they found that the rate of prediction was 88%. This prediction was dependent on the cutting parameters. When it came to the machining of Ti-6Al-4V alloy, Kosarac et al. [29] were able to accurately forecast the surface roughness with the RF model by using the cutting condition as input in addition to the process parameters with a limited data set. For their machine learning algorithms, Mazid et al. [30] employed the coating state of the cutting tool and the nose radius of the cutting tool as inputs. Additionally, they used process parameters. It has been discovered that the SVM method with radial basis function kernel (SVM-R) is quite suited for investigating the machining processes of Ti-6Al-4V alloy. This is in comparison to the SVM algorithm with a linear kernel, RF, DL, and ensemble approaches.

As can be seen from the paragraph above, although many studies have been published on surface roughness prediction using ML models in the machining of various materials, there are a limited number of studies on surface roughness prediction using ML and DL methods in the machining of stainless steels, which are difficult to cut and critical for surface quality. Table 1 shows studies on surface roughness prediction using ML and DL models in the machining of stainless steels. While the majority of studies focus on making predictions using cutting parameters, only Dubey et al. [35] made predictions by taking into account the size and concentration of nanoparticles in the nanofluid used in the N-MQL method. However, the importance of MQL and N-MQL parameters on surface quality is known. In the presented study, surface roughness was predicted for the first time using various ML models such as PR, SVR, DT, RF, and K-NN regression, depending on the cutting condition, MQL flow rate, nanoparticle concentration, cutting tool coating, and cutting temperature in the sustainable milling of AISI420 stainless steel using the MQL method using MWCNT-reinforced nanofluid.

Table 1. Studies on surface roughness prediction using ML/DL models in the SS machining

Study	Material	Method	Model(s)	ML/DL	Model inputs
Çaydaş et al. [31]	AISI 304	Turning	SVR ANN	ML	Cutting speed Feed rate Depth of cut
Zhou et al. [32]	AISI 304	Turning	GA-GBRT ANN SVR	ML	Cutting speed Feed rate Depth of cut
Vasanth et al. [33]	SS 410	Turning	ANN	ML	Cutting speed Feed rate Depth of cut
Du et al. [34]	Stainless Steel	Turning	PSD	ML	Spindle preload Temperature Cutting speed
Dubey et al. [35]	AISI 304	Turning	LR RF SVR	ML	Cutting speed Feed rate Depth of cut Nanoparticle concentration Nanoparticle size
Diren et al. [16]	Stainless Steel	Milling	ANN DT K-NN	ML	Cutting speed Feed rate Depth of cut
Huang et al. [36]	SUS 304	Turning	ANN	ML	Cutting speed Feed rate Depth of cut
Tsai et al. [37]	SUS 304	Milling	DNN CNN LSTM	DL	Cutting speed Feed rate Axial depth of cut Radial depth of cut
Bennet et al. [38]	AISI 316	Turning	GBRT	ML	Cutting speed Feed rate Depth of cut

Bober et al. [39]	AISI 304 AISI 304L	Turning	PR ANN	ML	Tensile strength Yield strength Elongation Hardness
Ross et al. [17]	AM-316L	Milling	TransGAN Alexnet	DL	Cutting condition Cutting speed Feed rate
Presented Study	**AISI 420**	**Milling**	**PR SVR DT RF K-NN**	**ML**	**Cutting condition Flow rate Nanoparticle concentration Cutting tool coating Cutting Temperature**

SVR: support vector regression, ANN: artificial neural network, GA-GBRT: genetic algorithim-gradient boosting regression tree, PSD: power spectral density LR: linear regression, RF: random forest, DT: decision tree, K-NN: k-nearest neighbor, DNN: deep neural network, CNN: convolutional neural network, LSTM: long short-term memory, PR: polynomial regression, TransGAN: generative adversarial networks with transformers, Alexnet: CNN architecture, designed by Alex Krizhevsky

2. MATERIAL AND METHOD

2.1. Experimental Study

2.1.1. Details of AISI 420 martensitic stainless-steel workpiece

In the present study, AISI 420 martensitic stainless steel (MSS), which is widely employed in various industrial applications, such as shafts, gears, springs, cutting blades, and other components requiring hardness, wear resistance, and mechanical strength, yet is known to exhibit poor machinability characteristics, was selected as the workpiece material [40]. The specimens were prepared in plate form with dimensions of 250 × 200 × 6 mm to ensure sufficient surface area and structural stability during the milling experiments the chemical composition of the AISI 420 MSS used in this study is presented in Table 2, while the corresponding mechanical properties are summarized in Table 3. These material properties were provided by the material supplier.

Table 2. Chemical compositions of AISI 420 MSS.

Cr %	C %	Si %	Mn %	P %	S %	Fe %
13.11	0.36	0.42	0.37	0.022	0.003	Rest

Table 3. Mechanical properties of AISI 420 MSS.

Yield Stress (MPa)	Tensile Stress (MPa)	Elongation (%)	Hardness (HRB)
245	655	25	95

2.1.2. Preparation of nanofluids

Within the scope of this study, a series of nano fluids were formulated by dispersing multi-walled carbon nanotubes (MWCNTs) into a commercial vegetable-based cutting oil, Eraoil KT/2000, at different weight fractions. Specifically, MWCNT concentrations of 0.1 wt.%, 0.15 wt.%, 0.2 wt.%, 0.5 wt.%, 1 wt.%, and 3 wt.% were selected in order to obtain nanofluids with varying solid loadings while preserving stable and uniform suspensions. The base fluid, Eraoil KT/2000, is characterized by its reddish appearance, a density of 0.85 g/cm³ at 20 °C, and a kinematic viscosity of 11 cSt at the same temperature, making it a suitable environmentally friendly lubricant for machining applications.

The MWCNTs employed for nanofluid preparation were from the NANOCYL™ NC7000 series, with a reported purity level of approximately 90%. These nanotubes exhibit an average outer diameter of 9.5 nm and an average length of about 1.5 μm, resulting in a high aspect ratio that is favorable for enhancing thermo-physical properties. In addition, the MWCNTs possess a specific surface area in the range of 250-300 m²/g, which facilitates effective interaction with the vegetable oil matrix. Owing to their exceptionally high thermal conductivity, reported to be on order of ~3000 W/mK, the incorporation of MWCNTs is expected to significantly influence the heat transfer characteristics of the resulting nanofluids. Accordingly, the prepared nano fluids with different MWCNT loadings provide a suitable basis for systematically evaluating the effect of nanoparticle concentration on the thermal and tribological performance of the cutting fluid.

The MWCNT nanoparticles were initially dried in an oven that was manufactured by Termal. This was done in order to eliminate any moisture that might have been present throughout the process. This was done in order to guarantee that the nanofluids that were prepared were consistent and homogenous. After that, a Radwag PS 510R digital precision balance was applied in order to include nanoparticles into the Eraoil KT/2000 cutting fluid in the quantities that were required. This was done in order to achieve the desired results. A precision balance was also utilized in order to add Sodium Dodecyl Sulfate (SDS) surfactant into the cutting oil at a ratio of 0.1% of the weights of the MWCNT nanoparticles. This was done in order to ensure that the cutting of oil was of the highest possible quality. Both the homogeneity of the mixtures and the amount of time that the mixtures were permitted to settle were improved as a result of this action, which was taken. In the end, a homogenous mixture was obtained by putting the commercial vegetable-based oil, MWCNT, and SDS mixture through a digital homogenizer of the Daihan WiseTis HG-15D brand at a speed of 5000 revolutions per minute for a duration of two hours. This process was repeated until the mixture was completely homogenized.

The incorporation of nanoparticles into vegetable-based oil is widely recognized to enhance the viscosity of the fluid, thus influencing the stability and lubricating properties of nanofluids [9]. The incorporation of nanoparticles into the lubricant results in an increase in the fluid's density and viscosity, as well as an increase in the thermal conductivity of the lubricant and the retention of the lubricant inside the cutting zone [41]. However, increasing the viscosity value more than necessary causes the nanoparticles to agglomerate, reduce the wettability and clog the MQL nozzle [42]. For these reasons, the viscosity values of the prepared nanofluids at room temperature were measured using the AND brand ST100 model viscosity determination device and the results are given in Table 4. Since the viscosity range in which the Werte DKN 25 MQL system used in the presented study can operate is 2-30 cst, nanofluids prepared at 0.5%, 1%, and 3% by weight were not used in the experiments.

Table 4. Viscosity measurement values of prepared nanofluids

Cutting Fluids	Viscosity (cst) at 20 °C
Pure vegatable cutting fluid	11
Pure vegatable cutting fluid + 0.1% wt. MWCNT	15.7
Pure vegatable cutting fluid + 0.15% wt. MWCNT	18.3
Pure vegatable cutting fluid + 0.2% wt. MWCNT	21.7
Pure vegatable cutting fluid + 0.5% wt. MWCNT	77.6
Pure vegatable cutting fluid + 1% wt. MWCNT	372
Pure vegatable cutting fluid + 3% wt. MWCNT	Solidification

2.1.3. Equipment and tools for experiments

The experimental configuration and the methodology followed in this study are schematically illustrated in Figure 1. All end milling experiments were carried out on a First brand MCV-300 CNC machining center, which provided stable cutting conditions throughout the tests. For the machining trials, SPHN 120404 tungsten carbide (WC) cutting inserts, used in either uncoated form or coated with titanium nitride (TiN), were mounted on a tool holder equipped with two inserts having a nominal diameter of 32 mm. The selected inserts were chosen in accordance with the manufacturer’s recommendations and also considering their suitability for the workpiece material and cutting conditions employed in this study. This tool configuration was selected to ensure repeatable cutting engagement and consistent chip formation during the milling operations.

Minimum quantity lubrication (MQL) experiments were performed using both the prepared nanofluids and the base vegetable cutting oil. The MQL application was supplied by a Werte DKN25 system, which delivers the lubricant in an atomized form directly to the cutting zone. The MQL nozzle had an orifice diameter of 1 mm and was positioned in the feed direction to maximize lubricant penetration into the tool–workpiece interface. The nozzle was maintained at a fixed stand-off distance of 50 mm from the cutting region and inclined at an angle of 10° relative to the workpiece surface in order to achieve consistent and effective lubrication during machining.

Cutting temperature measurements were conducted using an Optris CTlaser 3MH1 dual-laser, non-contact temperature measurement device. This system allows real-time monitoring of temperature without interfering with the cutting process. The acquired temperature data was processed and recorded using Compact Connect software installed on a computer. During the measurements, the laser beam was focused on the cutting tool tip, which is the region most directly affected by thermal loads, and temperature values were continuously captured throughout the cutting operation.

Surface roughness measurements of the machined surfaces were carried out using a Time brand TR200 portable surface roughness tester. The tester utilized a diamond-tipped stylus (5 μm curvature radius) moving at 0.4 mm/s. The sampling length (Ln) was set to 2.5 mm, while the cutoff length (λc) for the measurement was at 1.0 mm. To ensure measurement reliability and account for surface variability, roughness values were recorded ten times at different locations along the milled surface. The arithmetic mean of these ten measurements was calculated and reported as the representative surface roughness value for each experimental condition. This approach was adopted to minimize the influence of local surface irregularities and to provide a more robust assessment of surface quality.

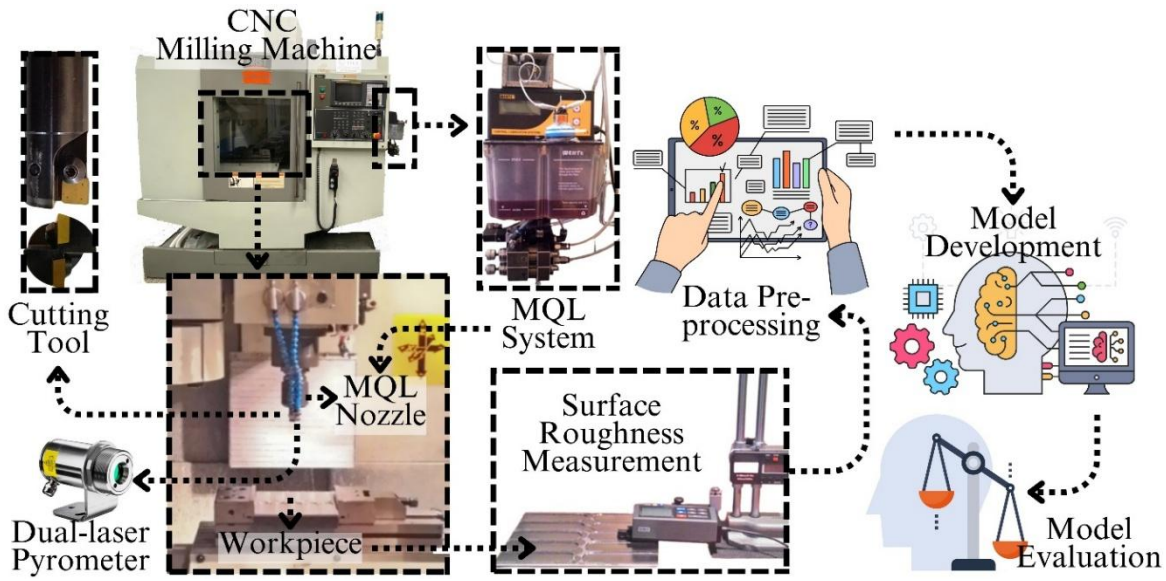


Figure 1. Experimental setup and procedure

2.1.4. Experimental plan

In the present investigation, the influence of various machining and lubrication-related parameters on surface roughness and cutting temperature during the milling of AISI 420 martensitic stainless steel (MSS) was systematically evaluated. The study considered different cutting environments, namely dry cutting, minimum quantity lubrication (MQL), and nanofluid-based minimum quantity lubrication (NMQL). In addition, the effect of MQL flow rate was examined at three levels (0, 20, and 40 mL/h), together with different nanoparticle weight concentrations (0, 0.1%, 0.15%, and 0.2%) and cutting tool conditions, including uncoated tungsten carbide (WC) and titanium nitride (TiN)-coated WC tools.

To isolate the effects of these variables and ensure experimental consistency, the primary cutting parameters were maintained at constant levels throughout all tests. Accordingly, the cutting speed was fixed at 100 m/min, the feed value at 0.18 mm/rev, and the depth of cut at 0.5 mm. The detailed experimental design and parameter combinations employed in the study are summarized in Table 5.

Each milling test was conducted for a total duration of 400 s, with the process being intermittently stopped at 40 s intervals. At the end of each interval, cutting temperature and surface roughness measurements were recorded. This stepwise measurement approach enabled the monitoring of the temporal evolution of thermal and surface integrity characteristics under different machining conditions. Experiments were performed in triplicate to ensure the reliability of the results, and the average results obtained are presented.

Table 5. Experimental plan

Exp No	Cutting Condition	Flow Rate (mL/h)	Concentration by wt. (%)	Cutting Tool
1	Dry	0	0	WC
2	Dry	0	0	TiN-WC
3	MQL	20	0	WC
4	MQL	20	0	TiN-WC
5	MQL	40	0	WC
6	MQL	40	0	TiN-WC
7	NMQL	20	0.1	WC
8	NMQL	20	0.15	WC

9	NMQL	20	0.2	WC
10	NMQL	20	0.1	TiN-WC
11	NMQL	20	0.15	TiN-WC
12	NMQL	20	0.2	TiN-WC
13	NMQL	40	0.1	WC
14	NMQL	40	0.15	WC
15	NMQL	40	0.2	WC
16	NMQL	40	0.1	TiN-WC
17	NMQL	40	0.15	TiN-WC
18	NMQL	40	0.2	TiN-WC

2.2. Data pre-processing

2.2.1. Data loading and segregation

The dataset comprised various machining parameters such as cutting speed (m/min), feed (mm/rev), depth of cut (mm), cutting condition, MQL flow rate (mL/h), nanoparticle concentration (wt%), cutting tool, and cutting temperature (°C), and the target variable surface roughness. The dataset was loaded into a Pandas data frame and separated into input features (independent variables) and target variables (surface roughness).

2.2.2. Label encoding

Some of the machining parameters, such as cutting conditions, were qualitative in nature. A label encoder model was depolyed to convert these qualitative data strings. This involved assigning a unique numerical label to each category within the qualitative variable.

2.2.3. Standard scaling normalization

To ensure the standardization of the dataset and mitigate the effects of varying scales among features, standard scaling normalization technique was used. This involved transforming each feature to have a mean of 0 and a standard deviation of 1. Mathematically, the standard scaling transformation for a feature x is given in Equation 1:

$$x_{scaled} = \frac{x - mean(x)}{std(x)} \tag{1}$$

Where *mean(x)* represents the mean value of the feature *x* and *std(x)* represents its standard deviation.

2.3. Model development

In this study the development of predictive models for surface roughness in machining processes using various regression algorithms. The models are trained on input parameters, including cutting speed, feed, depth of cut, cutting condition, MQL flow rate, nanoparticle concentration, cutting tool, and cutting temperature, to predict the output parameter, surface roughness.

2.3.1. Polynomial regression (PR)

The PR extends linear regression by fitting a polynomial function to the data instead of a straight line. The polynomial regression equation of degree d can be represented by Equation 2:

$$y = \beta_0 + \beta_1 x + \beta_2 x^2 + \cdots + \beta_d x^d + \epsilon \tag{2}$$

Where y is the predicted surface roughness, x is the input parameter, $\beta_0, \beta_1, \ldots, \beta_d$ are the coefficients of the polynomial equation, and ϵ is the error term. The polynomial regression model captures nonlinear relationships between the input parameters and the target variable by including higher-order terms ($x_2, x_3, \ldots, x_d$) in the equation [43].

2.3.2. Support vector regression (SVR)

The SVR is a regression technique based on support vector machines (SVM) that aims to find a hyperplane with the maximum margin while minimizing the error between the predicted and actual values. The SVR

model seeks to find the function f(x) that predicts the surface roughness y given the input parameters x such that:

$$y = f(x) + \epsilon \tag{3}$$

Where y is the predicted surface roughness, x is the input parameter, and ϵ is the error term. The function *f(x)* is represented as a linear combination of kernel functions applied to the input parameters. SVR utilizes a kernel function to map the input parameters into a higher-dimensional feature space, where a linear regression model is applied to find the optimal hyperplane that separates the data points with a margin of tolerance [44].

2.3.3. Decision tree regression (DT)

The DT partitions the feature space into regions and fits a simple model within each region. The prediction for a given input feature vector *X* is obtained by traversing the decision tree and determining the constant value associated with the leaf node corresponding to the region where *X* falls. The prediction is performed using the following relation as shown in Equation 4 below:

$$\hat{Y} = T(x) \tag{4}$$

Where $\hat{Y}$ is the predicted surface roughness. *T(X)* represents the traversal of the decision tree *T* to find the leaf node corresponding to the input feature vector *X*, and the value associated with that leaf node is the predicted surface roughness. The decision tree recursively splits the feature space based on the values of input features, with each split aiming to minimize the variance of the target variable within each region. This process results in a hierarchical structure of binary decisions, leading to a final prediction at the leaf nodes [45].

2.3.4. Random forest regression (RF)

The RF is an ensemble learning technique that combines multiple decision trees to improve prediction performance of the model. Each decision tree in the random forest is trained on a random subset of the training data and a random subset of the input features. The prediction for a given input feature vector *X* is obtained by aggregating the predictions of individual decision trees in the forest. The prediction is performed using the relation given in Equation 5.

$$\hat{Y} = \frac{1}{n}\sum_{i=1}^{n} T_i(x) \tag{5}$$

Where $\hat{Y}$ is the predicted surface roughness. *n* is the number of decision trees in the random forest. $T_i(X)$ represents the prediction of the ith decision tree T_i for the input feature vector *X*. The random forest regression model aggregates the predictions of multiple decision trees to reduce the variance and improve the robustness of the prediction. By averaging the predictions of individual trees, the random forest model tends to provide more stable and accurate predictions compared to a single decision tree. Additionally, the randomness introduced during the training process helps mitigate overfitting and captures diverse patterns in the data [46].

2.3.5. K-nearest neighbors regression (K-NN)

The K-NN regression is a non-parametric algorithm that predicts the target variable by averaging the values of its K-NN in the feature space. The prediction is performed using the relation given in Equation 6.

$$\hat{Y} = f(X) = \frac{1}{k}\sum_{i=1}^{k} Y_{neighbor,i} \tag{6}$$

Where, $\hat{Y}$ is the predicted surface roughness for the input feature vector *X*. $Y_{neighbor,i}$ represents the target value (surface roughness) of the i^{th}nearest neighbor to the input feature vector *X* in the training dataset. *k* as the number of nearest neighbors to consider. The K-NN algorithm computes the distance between the input feature vector *X* and each training feature vector X_i using a distance metrices (e.g., Euclidean distance). This then selects the k nearest neighbors based on these distances and averages their target values to make the final prediction. K-NN regression does not learn a specific model during the training phase; instead, it stores the entire training dataset and uses it during the prediction phase. This makes K-NN regression simple and easy to implement, but it may become computationally expensive for large datasets. Additionally, the choice of the

distance metric and the number of nearest neighbors (k) are critical parameters that affect the performance of the K-NN algorithm [47].

2.4. Model Evaluation

Model evaluation is crucial for assessing the performance of predictive models and determining their effectiveness in making accurate predictions In this section, evaluation metrics used to quantify the performance of regression models developed to predict surface roughness in machining processes are presented [48].

2.4.1. Coefficient of determination

The coefficient of determination, which is more frequently referred to as R^2 [49], is a statistical tool that determines the extent to which the input features can be used to predict the variation in the target variable, which in this case is surface roughness. It offers a measure of the degree to which the regression model is able to accurately represent the variability present in the data. The value of the R^2 score can range from 0 to 1, with a greater value indicating that the model has a better fit to the data. The value of R^2 is determined by applying the relationship described in Equation 7.

$$R^2 = 1 - \frac{\sum_{i=1}^{m}(Y_i - \hat{Y}_i)^2}{\sum_{i=1}^{m}(Y_i - \bar{Y})^2} \tag{7}$$

2.4.2. Mean squared error (MSE)

The MSE is a statistical metric that determines the average squared difference between the predictions made for the target variable and the actual values of the variable [50]. Specifically, it offers a quantitative measurement of the accuracy of the model, with lower MSE values indicating greater prediction performance. The MSE is determined by using the relationship that is presented in Equation 8.

$$\frac{1}{m}\sum_{i=1}^{m}\left(Y_i - \hat{Y}_i\right)^2 \tag{8}$$

2.4.3. Mean absolute error (MAE)

When comparing the actual values of the target variable to the projected values, the MAE is a measurement that determines the average absolute difference between the two. A measure of the accuracy of the model is provided by it, just like the MSE does; however, it is less susceptible to outliers than the MSE. The MAE is determined by using the relationship that is presented in Equation 9.

$$\frac{1}{m}\sum_{i=1}^{m}\left|Y_i - \hat{Y}_i\right| \tag{9}$$

2.4.4. Root mean squared error (RMSE)

The RMSE is a measure of the spread of prediction mistakes that is calculated by taking the square root of the mean squared error [51]. Additionally, it is frequently utilized for the purpose of quantifying the average magnitude of prediction mistakes, and it can be interpreted in the same units as the objective variable. In order to determine the RMSE, the relationship described in Equation 10 is utilized.

$$RMSE = \sqrt{MSE} \tag{9}$$

3. RESULTS AND DISCUSSION

3.1. Experimental results

3.1.1. Cutting temperature

Figure 2 shows the cutting temperatures after 400 seconds of machining obtained according to different cutting conditions, MQL flow rates, nanoparticle concentrations, and cutting tool coating conditions. In terms of cutting temperature, the worst case is to use an uncoated WC cutting tool under dry-condition, and the best cutting condition is to use a TiN-coated WC cutting tool, NMQL-conditioning containing 0.15% MWCNT by

weight, and a flow rate of 40 ml/h. There was a 25.3% improvement between the best condition and the worst condition.

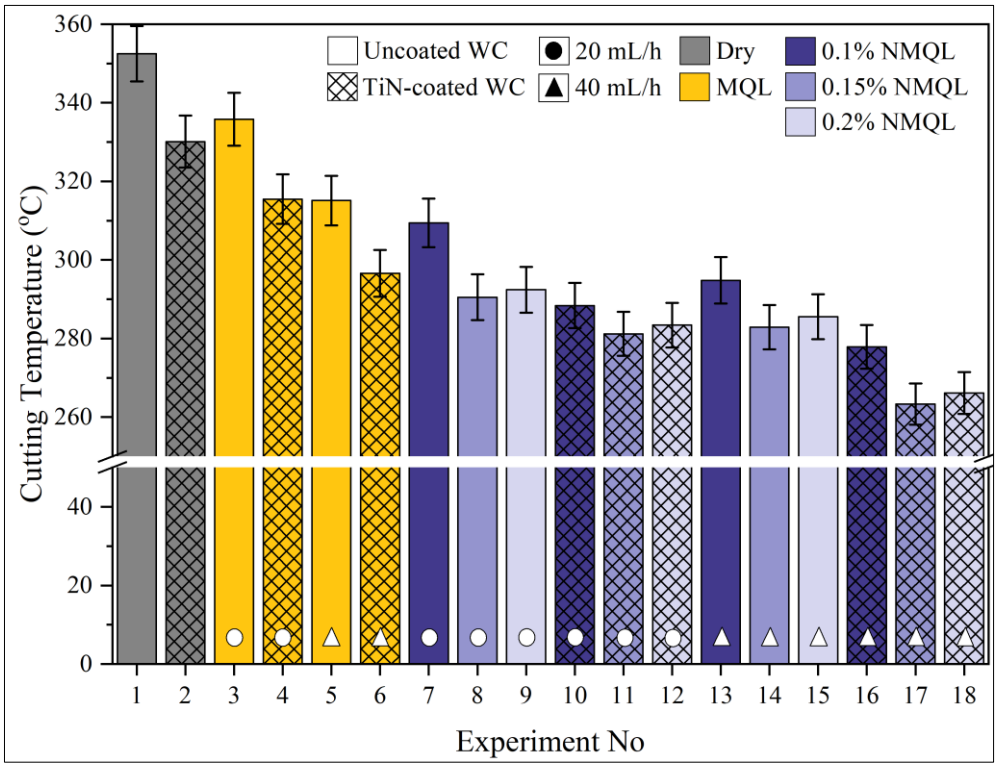


Figure 2. Cutting temperature results

It is known that cutting tool coatings reduce the cutting temperature through mechanisms such as the thermal barrier effect, reduction of tool-chip friction, modification of heat dissipation and coating thickness [52]. In this study, TiN-coated WC cutting tool improved the average cutting temperature by 5.7% compared to uncoated WC cutting tool. Coatings such as titanium nitride have significantly lower thermal conductivity than the tool substrate. This disparity creates a thermal barrier, which impedes the transfer of heat from the cutting zone to the tool substrate. As a result, the amount of heat penetrating the tool is reduced, thereby lowering the overall cutting temperature. Also, the presence of coatings decreases the coefficient of friction at the tool-chip interface. Lower friction means less heat is generated due to the reduced mechanical resistance between the tool and the material being cut. In addition, coatings modify the heat partition coefficient, which determines how heat is distributed between the tool and the chip. Effective coatings ensure that a smaller fraction of the generated heat is absorbed by the tool. Instead, more heat is carried away by the chip. This redistribution of heat is beneficial as it reduces the thermal load on the tool, maintaining a lower cutting temperature and preventing thermal damage to the tool.

According to the findings of an investigation into the impact of MQL flow rate on the cutting temperature, the utilization of flow rates of 20 mL/h and 40 mL/h, in comparison to the dry cutting condition, in which the MQL flow rate is zero, resulted in an average improvement of 12.2% and 16.4%, respectively, in the cutting temperature. A better lubrication, greater heat dissipation, and effective oil mist penetration are the physical mechanisms that are responsible for the improvement in cutting temperature that occurs when the MQL flow rate is increased [53]. When the flow rate of MQL is increased, there is a greater quantity of lubricants available at the cutting interface. The friction that occurs between the tool and the workpiece is reduced as a result, which results in lower temperatures. Additionally, the production of a lubricating film is positively impacted by increased MQL flow rates. The cutting zone is able to experience improved heat dissipation thanks to this film, which results in a decrease in the total temperature. In order to ensure that the oil mist is able to efficiently reach the cutting zone, higher flow rates are required, particularly when combined with air pressure that has been tuned. This enhanced penetration improves cooling efficiency, which in turn further reduces the temperatures at which cutting occurs.

If the effect of cutting conditions is analyzed, compared to dry cutting conditions, MQL and NMQL cutting conditions reduced the cutting temperature by 7.5% and 16.6%, on average, respectively. The reason for this situation is due to the improvement of the lubrication and thermal properties of the nanofluid prepared by adding MWCNT and SDS surfactant. The MWCNT lubrication mechanism in nanofluids is highly reliant on

the effective dispersion of MWCNTs, the formation of stable lubricating films, the rolling effect of the dispersed MWCNTs, and the synergistic interaction with surfactants that improve the overall tribological performance [54]. Additionally, due to the fact that MWCNT is more effective than other nanoparticles in enhancing thermal conductivity [55], the cutting heat that is produced in the cutting zone is quickly evacuated, which results in a drop in the cutting temperature.

When the effect of the MWCNT nanoparticle ratio used in the NMQL cutting condition on the cutting temperature was examined, the lowest cutting temperature was obtained when 0.15% by weight MWCNT was used. When compared to the dry method, the cutting temperatures were improved by 14.3%, 18.1%, and 17.4%, respectively, when the NMQL cutting conditions contained 0.1%, 0.15%, and 0.2% MWCNT by weight. It is well known that adding nanoparticles to vegetable oil increases the fluid's viscosity, which in turn affects the stability and lubricating properties of nanofluids [9]. The measured viscosity values of nanofluids containing 0.1%, 0.15% and 0.2% MWCNT by weight are 15.7, 18.3 and 21.7 cst, respectively. The lubricant's density and viscosity are increased when nanoparticles are added, and the lubricant's thermal conductivity and retention in the cutting zone are also increased [41]. However, increasing the viscosity value more than necessary causes the nanoparticles to agglomerate, reduce the wettability and clog the MQL nozzle [42]. For these reasons, the NMQL condition containing 0.15% MWCNT by weight provided a 3.9% improvement in cutting temperature compared to the one containing 0.2%.

3.1.2. Surface roughness

Figure 3 shows the surface roughness values after 400 second machining obtained according to different cutting conditions, MQL flow rates, nanoparticle concentrations, and cutting tool coating conditions. In terms of surface roughness, the worst case is to use an uncoated WC cutting tool under dry-condition, and the best cutting condition is to use a TiN-coated WC cutting tool under NMQL-condition containing 0.15% MWCNT by weight and a flow rate of 40 mL/h. There was a 49.9% improvement between the best condition and the worst condition.

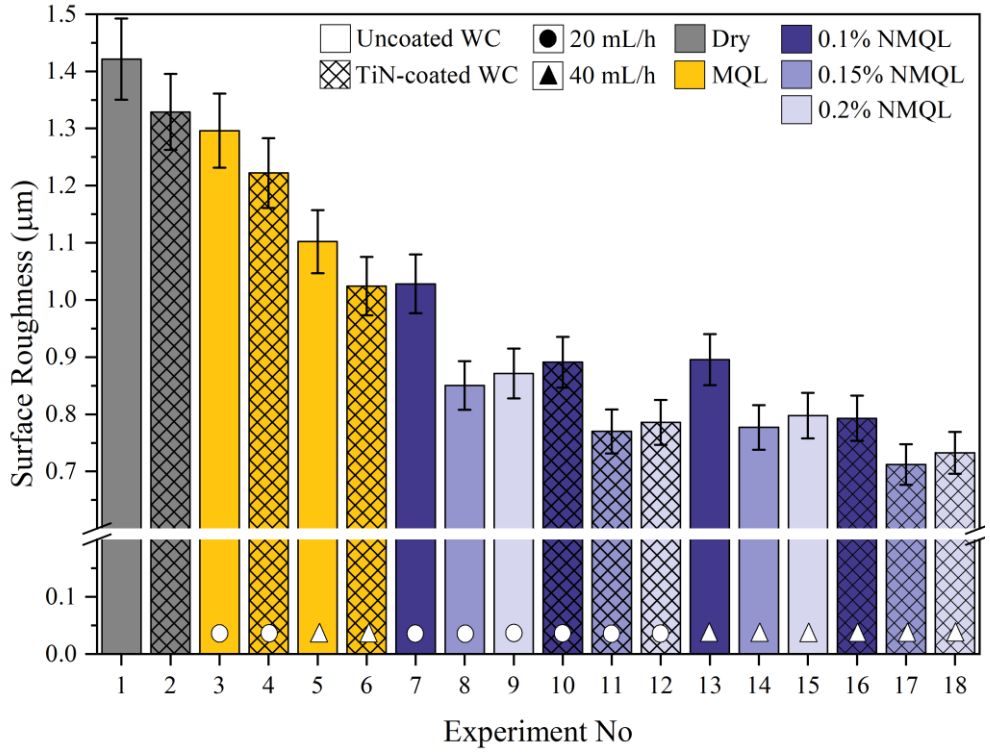


Figure 3. Surface roughness results.

The application of coatings on cutting tools results in improved surface roughness due to better wear resistance, reduced friction, enhanced thermal stability, reduced built-up edge (BUE), and leading to higher quality machined parts [56]. In this study, TiN-coated WC cutting tool improved the average surface roughness by 8.6% compared to uncoated WC cutting tool. Coatings reduce tool-chip friction during cutting and provide resistance to wear, thus less micro cracks and deformation occur in the workpiece [52]. This reduces final surface roughness, helping to obtain smoother and more precise surfaces. Also, coatings provide thermal stability that helps in maintaining the cutting-edge integrity at high temperatures [57]. This prevents thermal

degradation of the tool edge, leading to better surface quality. Coating reduces the tendency of material to adhere to the cutting edge, known as built-up edge (BUE) [52]. BUE can adversely affect the surface finish by causing roughness and irregularities. By minimizing BUE formation, coated tools help in achieving smoother surfaces. Also, it was shown by Seid Ahmed et al. [58] that coated cutting tools reduce BUE formation in the machining of stainless steels.

According to Mia et al. [59], MQL flow rate is one of the most effective factors affecting surface roughness rather than cutting speed and feed rate. Therefore, it is important to investigate the effect of MQL flow rates on surface roughness. In comparing the 20 mL/h and 40 mL/h MQL flow rates to the dry cutting condition (MQL flow rate is zero), the surface roughness was reduced by an average of 29.9% and 37.9%, respectively. Similar result was reported in machining AISI 202 stainless steel [60]. As the MQL flow rate increased, more lubricant droplets penetrated the cutting tool-workpiece interface, resulting in improved lubrication film, reduced friction, and ultimately reduced surface roughness [61].

Analyzing the effect of cutting conditions, it was determined that MQL and NMQL reduced surface roughness by an average of 15.6% and 40%, respectively, compared to unlubricated dry-cutting. The improvement in surface roughness that occurs when NMQL is utilized can be linked to a number of different mechanisms. These mechanisms include surface mending [62], protective film development [63], third body mechanism [64], rolling mechanism [65], and polishing effect [66] that are caused by the nanoparticles floating in the fluid.

The lowest surface roughness was achieved when 0.15% by weight MWCNT was utilized in the NMQL, according to an analysis of the impact of the MWCNT nanoparticle ratio on the surface roughness. In comparison to the dry cutting condition, the surface roughness values improved by 34.4%, 43.5%, and 42.1%, respectively, under NMQL cutting conditions that contained 0.1%, 0.15%, and 0.2% MWCNT by weight. The addition of nanoparticles to vegetable oil has a recognized impact on the stability and lubricating properties of nanofluids [9]. The density, viscosity, and lubricant retention in the cutting zone are all increased when nanoparticles are added to the lubricant [41], but excessive increases the wettability, reducing the lubrication performance, and agglomerated nanoparticles cause defects on the surface [42].

3.2. Comparison prediction results

This section reflects the results of the regression models developed for predicting surface roughness in machining processes, with 80% of the dataset used for training and 20% of the datset was reserved for testing. After training and testing the regression models using the specified methodology, the results given in Table 6 were obtained.

Table 6. Model evaluation results.

Regression Model	R^2 score	MSE	MAE	RMSE
PR (3^{rd} degree)	0.6457	0.0397	0.1993	0.1524
PR (5^{th} degree)	0.6823	0.0356	0.1470	0.1887
K-NN	0.9789	0.0023	0.0139	0.0483
DT	0.9302	0.0078	0.0229	0.0885
RF	0.9481	0.0057	0.0453	0.0758
SVR	0.6549	0.0382	0.1508	0.1954

Table 6 presents a comparative evaluation of the regression models employed in this study by reporting the R^2, MSE, MAE, and RMSE. These statistical indicators collectively provide a comprehensive assessment of each model's predictive capability and accuracy in estimating surface roughness during machining operations. An overall examination of the results indicates that the K-nearest neighbour (K-NN) regression model outperformed all other approaches. The K-NN model achieved the highest R^2 value of 0.9789, demonstrating an excellent level of agreement between the predicted and experimentally measured surface roughness values. In addition, this model exhibited the lowest error metrics among all the evaluated methods, with MSE, MAE, and RMSE values of 0.0023, 0.0139, and 0.0483, respectively. These low error values confirm the strong predictive accuracy and robustness of the K-NN model for the given dataset. The random forest (RF) regression model also showed a high predictive performance, yielding an R^2 score of 0.9481, which indicates a strong explanatory capability, albeit slightly inferior to that of the K-NN model. Similarly, the decision tree (DT)

regression model achieved a relatively high R^2 value of 0.9302, suggesting that tree-based learning methods are effective in capturing the nonlinear relationships between the input parameters and surface roughness. However, both RF and DT models produced higher error values compared to the K-NN model, reflecting comparatively reduced prediction precision. In contrast, the polynomial regression (PR) models demonstrated lower predictive performance. Among them, the third-degree polynomial regression exhibited the lowest R^2 value of 0.6457, indicating limited capability in explaining the variance in surface roughness. This model also resulted in relatively high MAE, MSE, and RMSE values of 0.1993, 0.0397, and 0.1524, respectively, highlighting its weaker prediction accuracy. Although the fifth-degree polynomial regression slightly improved the R^2 score to 0.6823, its overall performance remained inferior to that of the machine learning-based models. A similar trend was observed for the support vector regression (SVR) model, which achieved an R^2 value of 0.6549 and comparatively higher error metrics.

Figure 4 illustrates the comparison between the predicted surface roughness values ($\hat{Y}$) and the corresponding experimentally measured surface roughness values (Y) obtained from the testing dataset for each regression model.

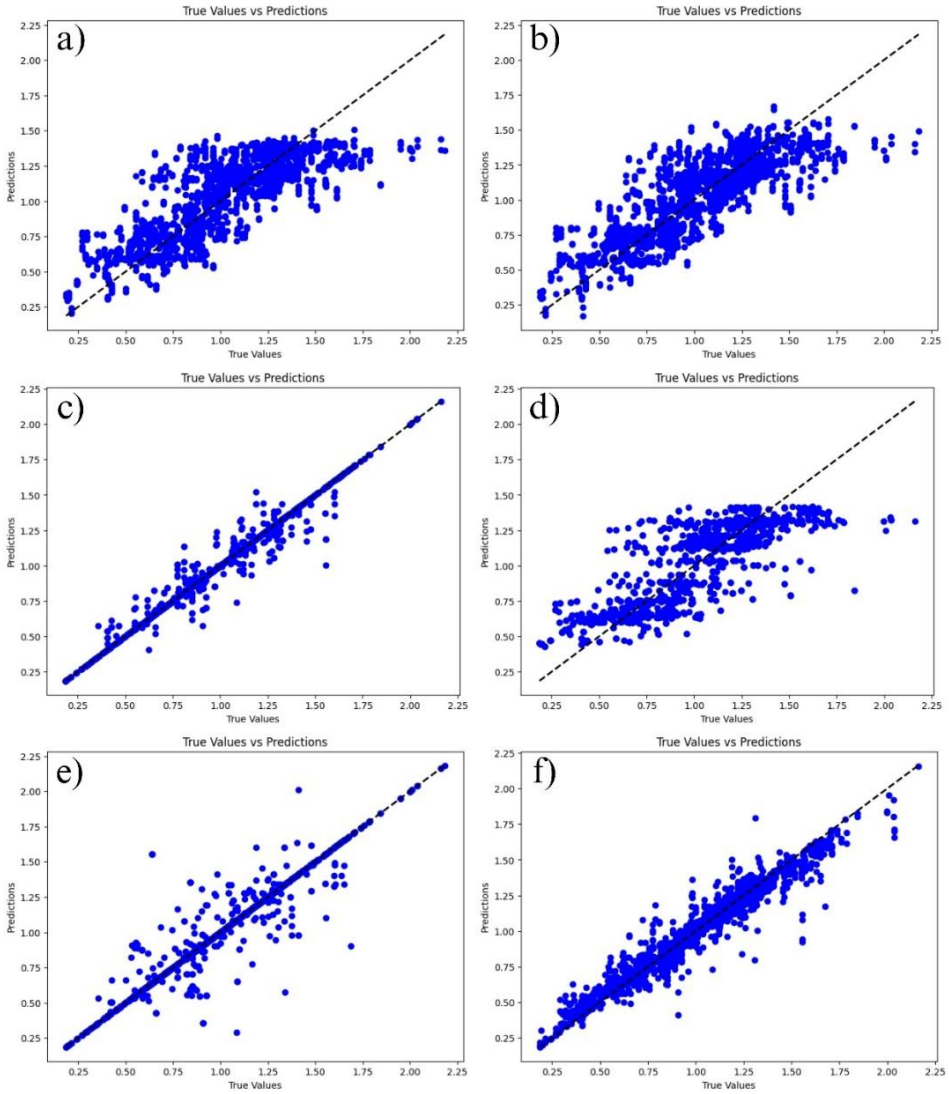


Figure 4. Graphs showing predicted surface roughness versus actual surface roughness: a) PR(3rd degree) b) PR(5th degree) c) K-NN d) SVR e) DT f) RF

These scatter plots provide a visual assessment of the predictive capability and reliability of the employed models. In each subplot, individual data points represent testing samples, while the dashed diagonal line (y = x) denotes the ideal case in which predicted values exactly match the measured values. A closer clustering of data points around the diagonal line indicates a higher level of prediction accuracy and a stronger agreement between the model outputs and experimental observations. In this regard, clear differences in predictive performance among the regression models can be observed. The K-NN and random forest models exhibit a pronounced alignment of data points along the diagonal, reflecting their superior ability to capture the

underlying relationships governing surface roughness. These models show relatively limited scatter and reduced deviation from the ideal prediction line, which is consistent with their high R^2 values and low error metrics. In contrast, the polynomial regression models of both third and fifth degree display a wider dispersion of points around the diagonal line, particularly at higher surface roughness values, indicating reduced prediction accuracy and a tendency toward systematic deviation. Similarly, the support vector regression and decision tree models demonstrate moderate performance, with noticeable scatter and localized deviations from the ideal line, suggesting a comparatively lower generalization capability for the given dataset.

In addition, Figure 5(a-f) provides a comparison between the experimental and predicted surface roughness values obtained from the different regression models, clearly revealing differences in their predictive capabilities.

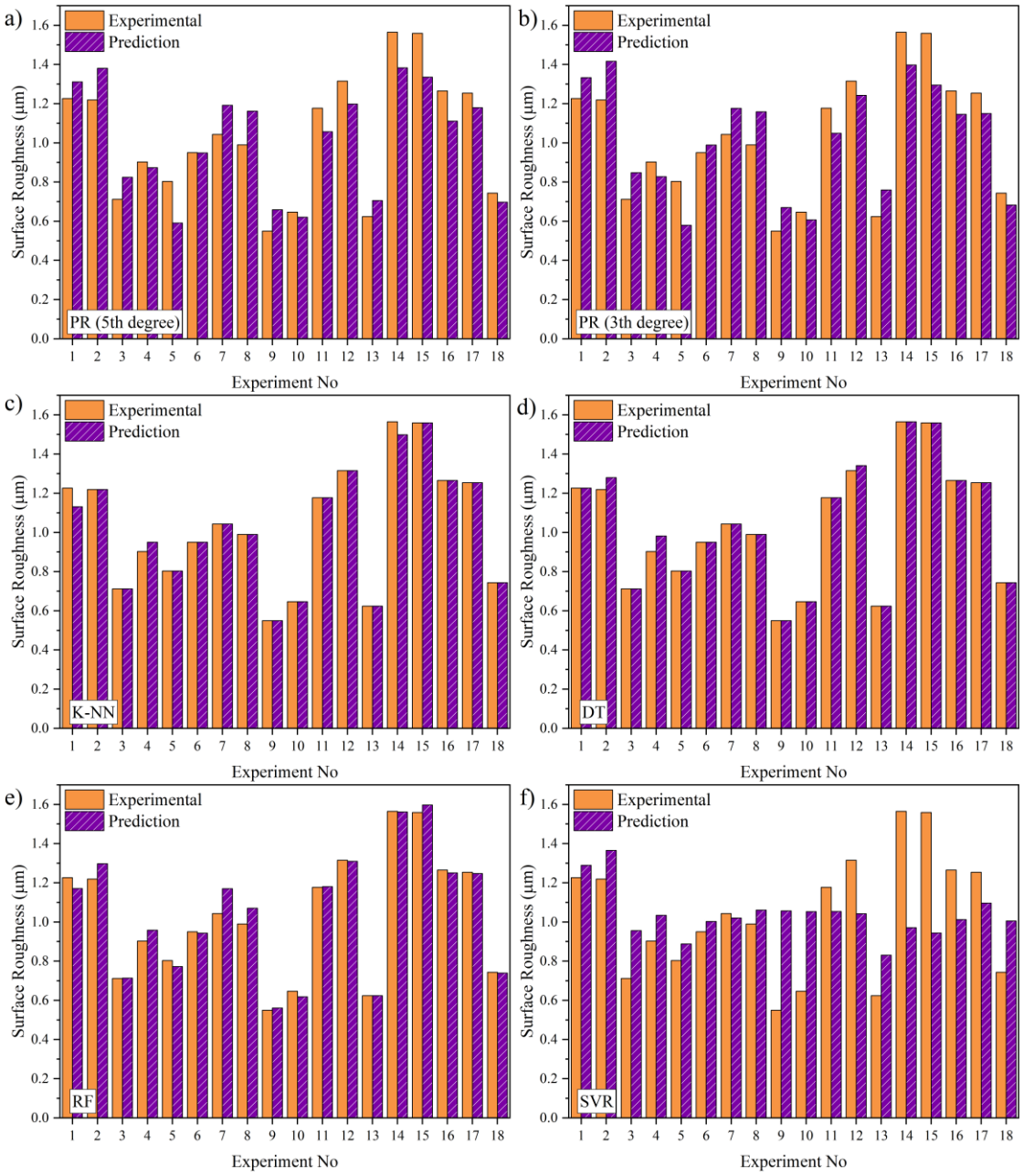


Figure 5. Comparison of experimental and predicted surface roughness results: a) PR(5^{th} degree) b) PR(3^{rd} degree) c) K-NN d) DT e) RF f) SVR

Among all models, K-NN demonstrated the closest agreement with experimental measurements, achieving an average percentage deviation of only 0.96% and a maximum deviation of 7.74% at Experiment No. 1. This is further supported by the highest R^2 score of 0.9789 and the lowest MSE (0.0023) and MAE (0.0139) values reported in Table 6. The DT model exhibited a similarly strong performance, with an average deviation of

0.87%, marginally lower than K-NN in terms of mean error, and a maximum deviation of 8.75% at Experiment No. 4, yielding an R^2 of 0.9302. The RF model also produced satisfactory predictions, with an average deviation of 3.01% and a maximum of 12.22% at Experiment No. 7, corresponding to an R^2 of 0.9481.

In contrast, the polynomial regression models showed notably lower predictive accuracy. PR-5th degree registered an average deviation of 11.31% and a peak error of 26.36% at Experiment No. 5, while PR-3rd degree performed slightly worse at 13.00% average deviation and 27.86% maximum error, also concentrated at Experiment No. 5, which corresponds to a relatively low surface roughness value of 0.803 μm, a region where polynomial models tend to extrapolate poorly. The SVR model exhibited the weakest overall performance, with an average percentage deviation of 25.32%, nearly three times higher than RF, and a striking maximum deviation of 92.20% at Experiment No. 9 (experimental value: 0.55 μm), indicating that SVR severely overestimates surface roughness at low-roughness conditions. This is also reflected in its R^2 score of 0.6549, the second lowest among all evaluated models.

The bar pairs for K-NN, DT, and RF align closely throughout all 18 experiments, including at both low-roughness (Exp. 9-13) and high-roughness (Exp. 14-15, ~1.56 μm) conditions, confirming robust generalization. Conversely, the PR and SVR bars exhibit systematic over- or under-prediction, particularly at the extremes of the roughness range. Overall, the results indicate that tree-based and instance-based machine learning models (K-NN, DT, RF) substantially outperform regression-based approaches (PR, SVR) in predicting surface roughness, with K-NN offering the best combination of accuracy and consistency across all experimental conditions.

4. CONCLUSIONS

In the presented study, surface roughness was predicted for the first time using various ML models such as PR, SVR, DT, RF, and K-NN, depending on the cutting condition, MQL flow rate, nanoparticle concentration, cutting tool coating, and cutting temperature in the sustainable milling AISI420 martensitic stainless steel using the MQL method using MWCNT-reinforced nanofluid. The conclusions obtained from the studies carried out are given below:

- TiN-coated WC cutting tool, NMQL method containing 0.15 wt.% MWCNT and 40 ml/h flow rate improved the cutting temperature by 25.3% compared to the dry cutting condition with the uncoated cutting tool.
- TiN-coated WC cutting tool, NMQL method containing 0.15 wt.% MWCNT and 40 ml/h flow rate reduced the surface roughness by 49.9% compared to the dry cutting condition with the uncoated cutting tool.
- The K-nearest neighbors regression ML (R^2 score of 0.9789) model outperformed other approaches in predicting surface roughness using inputs of cutting condition, MQL flow rate, nanoparticle concentration, cutting tool coating, and cutting temperature.
- Following K-NN, RF and DT effectively predicted the surface roughness by 95.81% and 93.02%, respectively. SVR and PR (3^{rd} and 5^{th} degree) failed to obtain accurate predictions.

This study derives the importance of prediction of surface roughness which indeed is necessary for looking after the product quality and better machining performance. In addition to testing different machine learning and/or deep learning models in future studies, MQL parameters such as nozzle distance and angle, which are known to influence surface roughness, will also be used as inputs in the models.

REFERENCES

[1] E. Dalibón, A. Dalke, H. Biermann, S.P. Brühl, Short time nitriding and nitrocarburizing of martensitic stainless steel, *Surf. Coat. Technol.* 485 (2024) 130931. https://doi.org/10.1016/j.surfcoat.2024.130931

[2] V. Rajkumar, N.S. Shanmugam, N.P. Kumar, K.K. Kumar, A.R. Kannan, Microstructure, mechanical properties, and corrosion behaviour of wire arc additive manufactured martensitic stainless steel 410 for pressure vessel applications, *Int. J. Press. Vessels Pip.* 209 (2024) 105171. https://doi.org/10.1016/j.ijpvp.2024.105171

[3] E. Saatçi, Y.F. Yapan, M. Uslu Uysal, A. Uysal, Orthogonal turning of AISI 310S austenitic stainless steel under hybrid nanofluid-assisted MQL and a sustainability optimization using NSGA-II and TOPSIS, *Sustain. Mater. Technol.* 36 (2023) e00628. https://doi.org/10.1016/j.susmat.2023.e00628

[4] A. Mohanty, S. Gangopadhyay, A. Thakur, On applicability of multilayer coated tool in dry machining of aerospace grade stainless steel, *Mater. Manuf. Process.* 31 (7) (2015) 869–879. https://doi.org/10.1080/10426914.2015.1070413

[5] P. Ranjan, S.S. Hiremath, Finite element simulation and experimental validation of machining martensitic stainless steel using multi-layered coated carbide tools for industry-relevant outcomes, *Simul. Model. Pract. Theory* 114 (2022) 102411. https://doi.org/10.1016/j.simpat.2021.102411
[6] G.M. Krolczyk, R.W. Maruda, J.B. Krolczyk, S. Wojciechowski, M. Mia, P. Nieslony, G. Budzik, Ecological trends in machining as a key factor in sustainable production – A review, *J. Clean. Prod.* 218 (2019) 601–615. https://doi.org/10.1016/j.jclepro.2019.02.017
[7] M.N. Babu, G. Manimaran, Experimental estimation of MQL in turning on AISI 410 stainless steel, *Int. J. Mach. Mach. Mater.* 19 (6) (2017) 522–537. https://doi.org/10.1504/IJMMM.2017.088894
[8] M.H.S. Elmunafi, D. Kurniawan, M.Y. Noordin, Use of castor oil as cutting fluid in machining of hardened stainless steel with minimum quantity of lubricant, *Procedia CIRP* 26 (2015) 408–411. https://doi.org/10.1016/j.procir.2015.03.001
[9] Ç.V. Yıldırım, S. Sirin, T. Kıvak, M. Sarıkaya, A comparative study on the tribological behavior of mono and proportional hybrid nanofluids for sustainable turning of AISI 420 hardened steel with cermet tools, *J. Manuf. Process.* 73 (2022) 695–714. https://doi.org/10.1016/j.jmapro.2021.11.044
[10] A. Hamdi, Y.F. Yapan, A. Uysal, et al., The effects of minimum quantity lubrication parameters on the lubrication efficiency in the turning of plastic mold steel, *Int. J. Adv. Manuf. Technol.* 132 (2024) 5803–5821. https://doi.org/10.1007/s00170-024-13706-5
[11] V.H. Nguyen, T.T. Le, Predicting surface roughness in machining aluminum alloys taking into account material properties, *Int. J. Comput. Integr. Manuf.* 37 (2024) 1–22. https://doi.org/10.1080/0951192X.2024.2372252
[12] L.C. Moreira, W.D. Li, X. Lu, M.E. Fitzpatrick, Supervision controller for real-time surface quality assurance in CNC machining using artificial intelligence, *Comput. Ind. Eng.* 127 (2019) 158–168. https://doi.org/10.1016/j.cie.2018.12.016
[13] P.G. Benardos, G.C. Vosniakos, Predicting surface roughness in machining: A review, *Int. J. Mach. Tools Manuf.* 43 (2003) 833–844. https://doi.org/10.1016/S0890-6955(03)00059-2
[14] R. Teti, D. Mourtzis, D.M. D'Addona, A. Caggiano, Process monitoring of machining, *CIRP Ann.* 71 (2022) 529–552. https://doi.org/10.1016/j.cirp.2022.05.009
[15] K. Ullrich, M. von Elling, K. Gutzeit, M. Dix, M. Weigold, J.C. Aurich, R. Wertheim, I.S. Jawahir, H. Ghadbeigi, AI-based optimisation of total machining performance: A review, *CIRP J. Manuf. Sci. Technol.* 50 (2024) 40–54. https://doi.org/10.1016/j.cirpj.2024.01.012
[16] D. Demircioglu Diren, N. Ozsoy, M. Ozsoy, Optimization of cutting parameters and result predictions with response surface methodology, individual and ensemble machine learning algorithms in end milling of AISI 321, *Arab. J. Sci. Eng.* 48 (2023) 12075–12089. https://doi.org/10.1007/s13369-023-07642-x
[17] N.S. Ross, P.M. Mashinini, C.S. Shibi, M.K. Gupta, M.E. Korkmaz, G.M. Krolczyk, V.S. Sharma, A new intelligent approach of surface roughness measurement in sustainable machining of AM-316L stainless steel with deep learning models, *Measurement* 230 (2024) 114515. https://doi.org/10.1016/j.measurement.2024.114515
[18] Y.S. Chuo, J.W. Lee, C.H. Mun, I.W. Noh, S. Rezvani, D.C. Kim, J. Lee, S.W. Lee, S.S. Park, Artificial intelligence enabled smart machining and machine tools, *J. Mech. Sci. Technol.* 36 (2022) 1–23. https://doi.org/10.1007/s12206-021-1201-0
[19] V. Nasir, F. Sassani, A review on deep learning in machining and tool monitoring: Methods, opportunities, and challenges, *Int. J. Adv. Manuf. Technol.* 115 (2021) 2683–2709. https://doi.org/10.1007/s00170-021-07325-7
[20] C. Prakasvudhisarn, S. Kunnapapdeelert, P. Yenradee, Optimal cutting condition determination for desired surface roughness in end milling, *Int. J. Adv. Manuf. Technol.* 41 (2009) 440–451. https://doi.org/10.1007/s00170-008-1491-8
[21] Z. Jurkovic, G. Cukor, M. Brezocnik, A comparison of machine learning methods for cutting parameters prediction in high speed turning process, *J. Intell. Manuf.* 29 (2018) 1683–1693. https://doi.org/10.1007/s10845-016-1206-1
[22] A. Yeganefar, S.A. Niknam, R. Asadi, The use of support vector machine, neural network, and regression analysis to predict and optimize surface roughness and cutting forces in milling, *Int. J. Adv. Manuf. Technol.* 105 (2019) 951–965. https://doi.org/10.1007/s00170-019-04227-7
[23] V.H. Nguyen, T.T. Le, H.S. Truong, M.V. Le, V.L. Ngo, A.T. Nguyen, H.Q. Nguyen, Applying Bayesian optimization for machine learning models in predicting the surface roughness in single-point diamond turning polycarbonate, *Math. Probl. Eng.* 2021 (2021) 6815802. https://doi.org/10.1155/2021/6815802
[24] A.T. Nguyen, V.H. Nguyen, T.T. Le, N.T. Nguyen, Multiobjective optimization of surface roughness and tool wear in high-speed milling of AA6061 by machine learning and NSGA-II, *Adv. Mater. Sci. Eng.* 2022 (2022) 5406570. https://doi.org/10.1155/2022/5406570
[25] Y. Zhang, X. Xu, Machine learning surface roughnesses in turning processes of brass metals, *Int. J. Adv. Manuf. Technol.* 121 (2022) 2437–2444. https://doi.org/10.1007/s00170-022-09498-1
[26] M.P. Motta, C. Pelaingre, A. Delamézière, L.B. Ayed, C. Barlier, Machine learning models for surface roughness monitoring in machining operations, *Procedia CIRP* 108 (2022) 710–715. https://doi.org/10.1016/j.procir.2022.03.110
[27] U.L. Adizue, A.D. Tura, E.O. Isaya, Surface quality prediction by machine learning methods and process parameter optimization in ultra-precision machining of AISI D2 using CBN tool, *Int. J. Adv. Manuf. Technol.* 129 (2023) 1375–1394. https://doi.org/10.1007/s00170-023-12366-1

[28] İ. Asiltürk, M. Kuntoğlu, R. Binali, H. Akkuş, E. Salur, A comprehensive analysis of surface roughness, vibration, and acoustic emissions based on machine learning during hard turning of AISI 4140 steel, *Metals* 13 (2023) 437. https://doi.org/10.3390/met13020437
[29] A. Kosarac, S. Tabakovic, C. Mladjenovic, M. Zeljkovic, G. Orasanin, Next-gen manufacturing: Machine learning for surface roughness prediction in Ti-6Al-4V biocompatible alloy machining, *J. Manuf. Mater. Process.* 7 (2023) 202. https://doi.org/10.3390/jmmp7060202
[30] A.M. Mazid, T. Imam, K.B. Ahsan, N. Khandoker, Characterising surface roughness of Ti-6Al-4V alloy machined using coated and uncoated carbide tools with variable nose radius by machine learning, *Eng. Appl. Artif. Intell.* 124 (2023) 106546. https://doi.org/10.1016/j.engappai.2023.106546
[31] U. Çaydaş, S. Ekici, Support vector machines models for surface roughness prediction in CNC turning of AISI 304 austenitic stainless steel, *J. Intell. Manuf.* 23 (2012) 639–650. https://doi.org/10.1007/s10845-010-0415-2
[32] T. Zhou, L. He, J. Wu, F. Du, Z. Zou, Prediction of surface roughness of 304 stainless steel and multi-objective optimization of cutting parameters based on GA-GBRT, *Appl. Sci.* 9 (2019) 3684. https://doi.org/10.3390/app9183684
[33] X.A. Vasanth, P.S. Paul, A.S. Varadarajan, A neural network model to predict surface roughness during turning of hardened SS410 steel, *Int. J. Syst. Assur. Eng. Manag.* 11 (2020) 704–715. https://doi.org/10.1007/s13198-020-00986-9
[34] C. Du, C.L. Ho, J. Kaminski, Prediction of product roughness, profile, and roundness using machine learning techniques for a hard turning process, *Adv. Manuf.* 9 (2021) 206–215. https://doi.org/10.1007/s40436-021-00345-2
[35] V. Dubey, A.K. Sharma, D.Y. Pimenov, Prediction of surface roughness using machine learning approach in MQL turning of AISI 304 steel by varying nanoparticle size in the cutting fluid, *Lubricants* 10 (2022) 81. https://doi.org/10.3390/lubricants10050081
[36] P.B. Huang, M.M.W. Inderawati, R. Rohmat, The development of an ANN surface roughness prediction system of multiple materials in CNC turning, *Int. J. Adv. Manuf. Technol.* 125 (2023) 1193–1211. https://doi.org/10.1007/s00170-022-10709-y
[37] M.H. Tsai, J.N. Lee, H.D. Tsai, M.J. Shie, T.L. Hsu, H.S. Chen, Applying a neural network to predict surface roughness and machining accuracy in the milling of SUS304, *Electronics* 12 (2023) 981. https://doi.org/10.3390/electronics12040981
[38] K.S. Bennett, J.M. DePaiva, S.C. Veldhuis, An integrated framework for a multi-material surface roughness prediction model in CNC turning using theoretical and machine learning methods, *Int. J. Adv. Manuf. Technol.* 131 (2024) 3579–3598. https://doi.org/10.1007/s00170-024-13201-x
[39] P. Bober, K. Zgodavová, M. Cicka, M. Mihaliková, J. Brindza, Predictive quality analytics of surface roughness in turning operation using polynomial and artificial neural network models, *Processes* 12 (2024) 206. https://doi.org/10.3390/pr12010206
[40] P. Ranjan, S.S. Hiremath, An experimental investigation on bio-inspired structure position variation on tool surface during turning of difficult to machine materials, *J. Mater. Eng. Perform.* 33 (2024) 5100–5119. https://doi.org/10.1007/s11665-023-08329-y
[41] M. Corcione, Empirical correlating equations for predicting the effective thermal conductivity and dynamic viscosity of nanofluids, *Energy Convers. Manag.* 52 (2011) 789–793. https://doi.org/10.1016/j.enconman.2010.06.072
[42] E. Şirin, T. Kıvak, Ç.V. Yıldırım, Effects of mono/hybrid nanofluid strategies and surfactants on machining performance in the drilling of Hastelloy X, *Tribol. Int.* 157 (2021) 106894. https://doi.org/10.1016/j.triboint.2021.106894
[43] E. Ostertagová, Modelling using polynomial regression, *Procedia Eng.* 48 (2012) 500–506. https://doi.org/10.1016/j.proeng.2012.09.545
[44] M. Awad, R. Khanna, Support vector regression, *Efficient Learning Machines: Theories, Concepts, and Applications for Engineers and System Designers* (2015) 67–80. https://doi.org/10.1007/978-1-4302-5990-9_4
[45] M. Xu, P. Watanachaturaporn, P.K. Varshney, M.K. Arora, Decision tree regression for soft classification of remote sensing data, *Remote Sens. Environ.* 97 (2005) 322–336. https://doi.org/10.1016/j.rse.2005.05.008
[46] V. Rodriguez-Galiano, M. Sanchez-Castillo, M. Chica-Olmo, M. Chica-Rivas, Machine learning predictive models for mineral prospectivity: An evaluation of neural networks, random forest, regression trees and support vector machines, *Ore Geol. Rev.* 71 (2015) 804–818. https://doi.org/10.1016/j.oregeorev.2015.01.001
[47] O. Kramer, Dimensionality reduction with unsupervised nearest neighbors, Springer, Berlin, 2013, pp. 13–23.
[48] D. Chicco, M.J. Warrens, G. Jurman, The coefficient of determination R-squared is more informative than SMAPE, MAE, MAPE, MSE and RMSE in regression analysis evaluation, *PeerJ Comput. Sci.* 7 (2021) e623. https://doi.org/10.7717/peerj-cs.623
[49] A.C. Cameron, F.A. Windmeijer, An R-squared measure of goodness of fit for some common nonlinear regression models, *J. Econom.* 77 (1997) 329–342. https://doi.org/10.1016/S0304-4076(96)01818-0
[50] A. De Myttenaere, B. Golden, B. Le Grand, F. Rossi, Mean absolute percentage error for regression models, *Neurocomputing* 192 (2016) 38–48. https://doi.org/10.1016/j.neucom.2015.12.114
[51] H. Zare Abyaneh, Evaluation of multivariate linear regression and artificial neural networks in prediction of water quality parameters, *J. Environ. Health Sci. Eng.* 12 (2014) 1–8. https://doi.org/10.1186/2052-336X-12-40

[52] J. Zhao, Z. Liu, B. Wang, J. Hu, Y. Wan, Tool coating effects on cutting temperature during metal cutting processes: Comprehensive review and future research directions, *Mech. Syst. Signal Process.* 150 (2021) 107302. https://doi.org/10.1016/j.ymssp.2020.107302

[53] F. Du, L. He, T. Zhou, P. Tian, Z. Zou, X. Zhou, Analysis of droplet characteristics and cooling lubrication effects in MQL milling of 316L stainless steel, *J. Mater. Res. Technol.* 19 (2022) 4832–4856. https://doi.org/10.1016/j.jmrt.2022.06.132

[54] T. Gao, C. Li, Y. Zhang, M. Yang, D. Jia, T. Jin, Y. Hou, R. Li, Dispersing mechanism and tribological performance of vegetable oil-based CNT nanofluids with different surfactants, *Tribol. Int.* 131 (2019) 51–63. https://doi.org/10.1016/j.triboint.2018.10.025

[55] Y. Hwang, J.K. Lee, C.H. Lee, Y.M. Jung, S.I. Cheong, C.G. Lee, B.C. Ku, S.P. Jang, Stability and thermal conductivity characteristics of nanofluids, *Thermochim. Acta* 455 (2007) 70–74. https://doi.org/10.1016/j.tca.2006.11.036

[56] A.A. Seenath, A.A.D. Sarhan, A state-of-the-art review on cutting tool materials and coatings in enhancing the tool performance in machining the superior nickel-based superalloys, *Arab. J. Sci. Eng.* (2024). https://doi.org/10.1007/s13369-024-08745-9

[57] K.D. Bouzakis, E. Bouzakis, S. Kombogiannis, S. Makrimallakis, G. Skordaris, N. Michailidis, P. Charalampous, R. Paraskevopoulou, R. M'Saoubi, J.C. Aurich, F. Barthelmä, D. Biermann, B. Denkena, D. Dimitrov, S. Engin, B. Karpuschewski, F. Klocke, T. Özel, G. Poulachon, J. Rech, V. Schulze, L. Settineri, A. Srivastava, K. Wegener, E. Uhlmann, P. Zeman, Effect of cutting edge preparation of coated tools on their performance in milling various materials, *CIRP J. Manuf. Sci. Technol.* 7 (2014) 264–273. https://doi.org/10.1016/j.cirpj.2014.05.003

[58] Y.S. Ahmed, J.M. Paiva, D. Covelli, S.C. Veldhuis, Investigation of coated cutting tool performance during machining of super duplex stainless steels through 3D wear evaluations, *Coatings* 7 (2017) 127. https://doi.org/10.3390/coatings7080127

[59] M. Mia, M.A. Bashir, M.A. Khan, et al., Optimization of MQL flow rate for minimum cutting force and surface roughness in end milling of hardened steel (HRC 40), *Int. J. Adv. Manuf. Technol.* 89 (2017) 675–690. https://doi.org/10.1007/s00170-016-9080-8

[60] J.S. Dureja, R. Singh, T. Singh, et al., Performance evaluation of coated carbide tool in machining of stainless steel (AISI 202) under minimum quantity lubrication (MQL), *Int. J. Precis. Eng. Manuf. Green Technol.* 2 (2015) 123–129. https://doi.org/10.1007/s40684-015-0016-9

[61] D.B. Cönger, Y.F. Yapan, U. Emiroğlu, A. Uysal, E. Altan, Influence of singular and dual MQL nozzles on sustainable milling of Al6061-T651 in different machining environments, *J. Manuf. Process.* 109 (2024) 524–536. https://doi.org/10.1016/j.jmapro.2023.12.043

[62] A.K. Sharma, A.K. Tiwari, A.R. Dixit, Mechanism of nanoparticles functioning and effects in machining processes: A review, *Mater. Today Proc.* 2 (2015) 3539–3544. https://doi.org/10.1016/j.matpr.2015.07.331

[63] M. Jamil, N. He, W. Zhao, et al., Tribology and machinability performance of hybrid Al_2O_3–MWCNTs nanofluids-assisted MQL for milling Ti-6Al-4V, *Int. J. Adv. Manuf. Technol.* 119 (2022) 2127–2144. https://doi.org/10.1007/s00170-021-08279-6

[64] D. Zhou, C. Li, K. You, K. Bi, Superlubricity transition from ball bearing to nanocoating in the third-body lubrication, *Tribol. Int.* 181 (2023) 108320. https://doi.org/10.1016/j.triboint.2023.108320

[65] A. Yücel, Ç.V. Yıldırım, M. Sarıkaya, Ş. Şirin, T. Kıvak, M.K. Gupta, İ.V. Tomaz, Influence of MoS_2 based nanofluid-MQL on tribological and machining characteristics in turning of AA 2024-T3 aluminum alloy, *J. Mater. Res. Technol.* 15 (2021) 1688–1704. https://doi.org/10.1016/j.jmrt.2021.09.007

[66] O. Öndin, T. Kıvak, M. Sarıkaya, Ç.V. Yıldırım, Investigation of the influence of MWCNTs mixed nanofluid on the machinability characteristics of PH 13-8 Mo stainless steel, *Tribol. Int.* 148 (2020) 106323. https://doi.org/10.1016/j.triboint.2020.106323